

High spin baryon in hot strongly coupled plasma

Miao Li ^{a,b *}, Yang Zhou ^{a,b†} and Push Pu ^{c‡}

^a *Interdisciplinary Center of Theoretical Studies, University of Science
and Technology of China, Anhui 230026, China*

^b *Institute of Theoretical Physics, Academia Sinica, Beijing 100080, China*

^c *Department of Modern Physics, University of Science and Technology of China,
Anhui 230026, China*

Abstract

We consider a string junction configuration of baryon in the finite-temperature supersymmetric Yang-Mills dual of the AdS-Schwarzschild black hole background. In particular, we investigate the screening length for high spin baryon composed of rotating N_c heavy quarks. To rotate quarks by finite force, we put hard infrared cutoff in the bulk and give quarks finite mass. We find that N_c microscopic strings are embedded reasonably in the bulk geometry when they have finite angular velocity ω , similar to the meson case. By defining the screening length as the critical separation of quarks, we compute the ω dependence of the baryon screening length numerically and obtain a reasonable result which shows that high spin baryons dissociate more easily. Finally, we discuss the Regge-like behaviors of baryon.

*E-mail: mli@itp.ac.cn

†E-mail: yzhou@itp.ac.cn

‡E-mail: sldvm@mail.ustc.edu.cn

Contents

1	Introduction	1
1.1	Meson in strongly coupled gauge field	2
1.2	Baryon in strongly coupled gauge field	2
2	Baryon configuration	3
3	ω dependence of the screening length	5
4	High spin baryon at nonzero temperature	9
5	Discussion and Conclusion	15

1 Introduction

Recently there has been much interest in studying strongly coupled QCD in terms of AdS/CFT correspondence. The first example of AdS/CFT correspondence is provided by the duality between the classical gravity in $\text{AdS}_5 \times \text{S}^5$ and $\mathcal{N} = 4$ supersymmetric Yang-Mills theory [1]. Quarks can be introduced as fundamental, light ones, which appear in the action. And they also can be introduced as external probes, which are often infinitely heavy and not included in the action. In the first case we need introduce the flavor branes, and the new background geometry is dual to supersymmetric $\text{SU}(N_c)$ Yang-Mills theory with N_f additional hypermultiplets [15]. In this paper we just treat the heavy quarks as probes. Since QCD is confining, we always consider a quark and an antiquark. To measure the interaction potential between two such quarks, we choose a physical, gauge invariant object named Wilson loop

$$W[C] = \text{tr} P \exp \int i A_\mu dx^\mu . \quad (1.1)$$

By choosing the contour C as a rectangle with length of \mathcal{T} in the time direction and two sides L in a space direction. When $L \ll \mathcal{T}$, we can extract the potential $V_{q\bar{q}}(L)$ by

$$\langle W(C) \rangle_0 = \exp(-V_{q\bar{q}}(L)\mathcal{T}) . \quad (1.2)$$

In the SYM at zero temperature, the potential between probe quark antiquark pair separated by L is given by [3, 2]

$$V_{q\bar{q}}(L) = -\frac{4\pi^2}{\Gamma(1/4)^4} \frac{\sqrt{2g_{YM}^2 N}}{L} \quad (1.3)$$

valid in the large N_c and large λ limit. In AdS/CFT framework, we obtain the potential by computing the action of the hanging string with the infinite boundary C of world sheet.

The dual gravity background of the SYM gauge theory at a nonzero temperature is the AdS metric with a black hole. The potential between two quarks then becomes [4]

$$V(L, T) \approx \sqrt{\lambda} f(L, T) (L < L_c) \quad V(L, T) \approx \lambda^0 g(L, T) (L > L_c), \quad (1.4)$$

where L_c is a critical separation, at which the qualitative behavior of the interaction potential between the quark and antiquark changes. Roughly speaking, when $L < L_c$, the quark and antiquark form a bound state and when $L > L_c$, the quark and antiquark interact weakly relatively. In hot plasma, the critical length is related to the temperature.

1.1 Meson in strongly coupled gauge field

We consider the quark-antiquark bound state as a meson and define $L_s = L_c$ as the meson screening length, which is the critical distance between the quark antiquark pair. Since at L_s separation, the qualitative behavior of the interaction potential changes. It is also considered that meson dissociation happens when the quark antiquark separation is larger than L_s . For example, once the screening length at a certain temperature is smaller than the radius of meson (such as the J/ψ) in the quark gluon plasma, the quarkonium will dissociate. The dissociation of meson can be used as the signal of the formation of QGP as well as its temperature profile. L_s can be expressed as a decreasing function of temperature and we usually write $L_s = \alpha/T_{diss}$ in hot plasma, where T_{diss} is the dissociation temperature, and α is a constant defined by the characteristic QCD plasma. Lattice calculations give more details of the static potential between a heavy quark and antiquark in hot QCD [6, 5]. But the potential between moving or rotating quarks is hard to calculated in lattice.

In recent work [7, 8], the meson screening length is analyzed in the case of a moving quark-antiquark pair. The velocity dependence of the screening length have been calculated.

$$L_s(v, T) \simeq L_s(0, T)(1 - v^2)^{1/4} \propto \frac{1}{T_{diss}}(1 - v^2)^{1/4}. \quad (1.5)$$

From this equation, we see the meson can not run too fast in order to avoid dissociation. At a certain temperature, the limiting velocity can be obtained by calculating the dispersion relation of mesons which are described as fluctuation of the flavor brane in the dual gravity background [9].

By studying the spectral function of meson fluctuation on the embedded flavor branes, we can obtain more information about the phase diagram for the strongly coupled gauge theory. The investigation can be extended to more realistic gauge/gravity frame, such as models with finite chemical potential, isospin density, or the Sakai-Sugimoto model [10]. High spin meson can be described as a rotating string in the gravity background [11, 12, 13].

1.2 Baryon in strongly coupled gauge field

Baryon has a configuration composed of N_c fundamental strings with the same orientation, which begin at the heavy quarks on the boundary and end on the wrapped brane on the

junction vertex in the AdS_5 [16]. In the baryon configuration of a very recent work [14], a D5 brane fills the S^5 which sits a point in AdS_5 . A simple action of the hanging string and vertex brane was proposed and the moving velocity dependence of baryon screening length was calculated, which is similar to the meson case.

In this paper, we consider the string junction configuration of baryon in the finite temperature supersymmetric Yang-Mills dual of the AdS-Schwarzschild black hole background. In particular, we investigate the screening length for the high spin baryon composed of rotating N_c heavy quarks. To rotate the heavy quarks by a finite force, we put hard infrared cutoff in the bulk and give the quark finite mass. We find that N_c macroscopic strings are embedded reasonably in the bulk gravity with angular velocity ω , similar to the meson case. By defining the screening length as the critical separation of quarks when the connecting string becomes close to the horizon, we compute the ω dependence of the screening length and find that the rotating quarks can dissociate more easily because of the centrifugal force. In section 2, we analyze the baryon configuration in the simplest geometry background, and find the string-brane representation of the high spin baryon in the bulk gravity. In section 3, we find the interesting trajectory of strings in bulk space with angular velocity ω and define the screening length of baryon using the usual method in hot plasma. Then we analyze the interaction potential between the quarks and show the critical behavior at the screening length. Finally we get a reasonable ω dependence of baryon screening length. In section 4, we relate the angular momentum J of the strings to the high spin of the baryon. We pick up the stable baryon configurations with different ω . The energy and J charge of the baryon are defined and the Regge-like behaviors of baryon were shown.

2 Baryon configuration

We analyze a baryon composed of N_c probe heavy quarks in the SYM plasma at nonzero temperature. While on the supergravity side, there are N_c fundamental strings with the same orientation, which begin at the heavy quarks on the boundary and end on the junction vertex in the AdS_5 . To give the quarks finite ω , we need to give them a finite mass scale at first, which means that we should put a infrared cutoff in the bulk. We denote the boundary radius r_Λ , then a free quark mass can be given as

$$m_q = \frac{1}{2\pi\alpha'}(r_\Lambda - r_0) . \quad (2.1)$$

where the $\frac{1}{2\pi\alpha'}$ is the string tension and r_0 is the black hole horizon. The free quark can be introduced as a string lying in the radial direction from the boundary to the horizon. Also, infrared cutoff in the bulk can be realized by introducing a single brane, but for simplicity we just ignore the backreaction and the dynamic of the boundary brane in our paper. The vertex is a D5 brane wrapped on the S^5 which sits the same point in the AdS_5 . And the strings also sit the same point in the S^5 .

The dual background $\text{AdS}_5 \times S^5$ metric with a black hole:

$$ds^2 = -f(r)dt^2 + \frac{r^2}{R^2}d\vec{x}^2 + \frac{dr^2}{f(r)} + R^2d\Omega_5^2, \quad (2.2)$$

where

$$f(r) = \frac{r^2}{R^2} \left(1 - \frac{r_0^4}{r^4} \right). \quad (2.3)$$

and R is the curvature radius of the AdS metric, r is the coordinate of the 5th dimension of AdS_5 and r_0 is the position of the black hole horizon, $d\Omega_5^2$ is the metric for a unit S_5 . The temperature of the gauge theory is given by the Hawking temperature of the black hole, $T = r_0/(\pi R^2)$. The gauge theory parameters N_c and λ are given by

$$\sqrt{\lambda} = \frac{R^2}{\alpha'} , \quad \frac{\lambda}{N_c} = g_{\text{YM}}^2 = 4\pi g_s , \quad (2.4)$$

where g_s is the string coupling constant and $\frac{1}{2\pi\alpha'}$ is the string tension. Infinite N_c and large λ correspond to large string tension and weak string coupling and thus justify the classical gravity treatment. We define the dimensionless quark mass

$$M_q = \frac{m_q}{T} = \frac{(r_\Lambda - r_0)R^2}{2\alpha'r_0} = \sqrt{\lambda} \frac{r_\Lambda - r_0}{2r_0}. \quad (2.5)$$

When the quarks move in hot plasma, the plasma is like wind if we still stand in the rest frame of the quarks. The boosted metric can be used to calculate the velocity dependence of the screening length [14]. In our paper, we consider quarks rotating in the $x_1 - x_2$ plane, the background metric can be written as

$$ds^2 = -f(r)dt^2 + \frac{r^2}{R^2}dx_3^2 + \frac{r^2}{R^2}(d\rho^2 + \rho^2d\theta^2) + \frac{1}{f(r)}dr^2 + R^2d\Omega_5^2 \quad (2.6)$$

where ρ and θ are the coordinates in $x_1 - x_2$ plane.

Now, we consider the rotating strings configuration corresponding the baryon with high spin. It is composed of N_c rotating quarks arranged in a circle on the boundary. For simplicity, we define the same angular velocity of N_c strings as constant ω . The axis lies along radial direction of the AdS and passes through the central of the boundary circle. Then, we parametrize one of N_c string as

$$\tau = t, \quad \sigma = r, \quad \theta = \omega t, \quad \rho = \rho(r). \quad (2.7)$$

For symmetry, N_c strings have the same embedding function $\rho(r)$. The single string Nambu-Goto action is

$$S_{\text{string}} = \frac{1}{2\pi\alpha'} \int d\sigma d\tau \sqrt{-\det[h_{ab}]}, \quad (2.8)$$

where $h_{ab} = g_{\mu\nu} \frac{\partial x^\mu}{\partial \sigma^a} \frac{\partial x^\nu}{\partial \sigma^b}$. We consider zero moving velocity but finite rotating speed. The velocity in x_3 direction dependence of the baryon property can be read from [14]. The induced metric on the world sheet h_{ab} is time independent, and the action can be written as

$$S_{\text{string}} = \frac{\mathcal{T}}{2\pi\alpha'} \int_{r_e}^{r_\Lambda} dr \sqrt{-\left(\frac{r^2}{R^2}\rho^2\omega^2 - f(r)\right) \left(\frac{1}{f(r)} + \frac{r^2}{R^2}\rho'^2(r)\right)}, \quad (2.9)$$

where \mathcal{T} is the total time. The action for the D5 brane can be written as [14]

$$S_{D5} = \frac{\mathcal{V}(r_e)\mathcal{T}V_5}{(2\pi)^5\alpha'^3}, \quad (2.10)$$

where V_5 is the volume of the compact brane and $\mathcal{V}(r_e) = \sqrt{-g_{00}}$ is the potential for the brane located at $r = r_e$. Since the D5 brane sits at a point in the AdS space, we ignore the ω dependence of the S_{D5} .

The total action of the system is then

$$S_{total} = \sum_{i=1}^{N_c} S_{string}^{(i)} + S_{D5}, \quad (2.11)$$

where we can consider only one typical string to get N_c strings' action for symmetry. We find static baryon configuration through extremizing S_{total} , first with respect to the $\rho(r)$ (we ignore the x_3 and θ for symmetry) that describe the embedding of the N_c strings and second with respect to $\rho(r_e)$ and r_e , the location of the vertex brane.

Generally, extremizing S_{total} with respect to $\rho(r_e)$ and r_e yields the $x_1 - x_2$ plane and r directions force balance condition (FBC). Since the system is axial symmetric, the coordinate of baryon vertex in \vec{x} direction $\rho(r_e)$ is static and treated as original point in the $x_1 - x_2$ plane. But bulk coordinate r_e is nonzero and believed to be dependent on ω .

As above, we get the radial FBC by extremizing S_{total} with respect to r_e

$$\sum_{i=1}^{N_c} H^{(i)} \Big|_{r_e} = \Sigma, \quad (2.12)$$

where

$$H^{(i)} \equiv \mathcal{L}^{(i)} - \rho'^{(i)} \frac{\partial \mathcal{L}^{(i)}}{\partial \rho'^{(i)}}, \quad (2.13)$$

$$\Sigma \equiv \frac{2\pi\alpha'}{\mathcal{T}} \frac{\partial S_{D5}}{\partial r_e} = \frac{V_5}{(2\pi)^4\alpha'^2} \frac{\partial \mathcal{V}(r_e)}{\partial r_e}, \quad (2.14)$$

In the following section, we will find the shape of the hanging strings in the rotating case and the relation between quark separation l_q and r_e change a lot when we increase the ω from zero. The ω dependence of the embedding function $\rho(r)$ and the spin dependence of baryon screening length will have apparent physical explanation.

3 ω dependence of the screening length

To find the static baryon configuration, we extremize S_{total} with respect to the function $\rho(r)$ describing the trajectories of the N_c strings in AdS. The world sheet lagrange density with parameters in (2.7) is

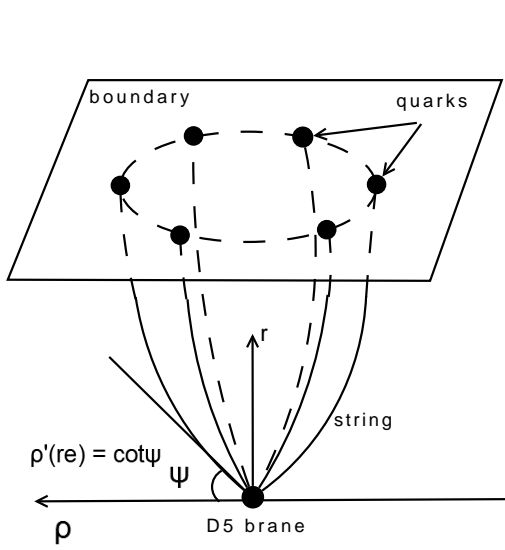


Figure 1: String-brane representation of baryon

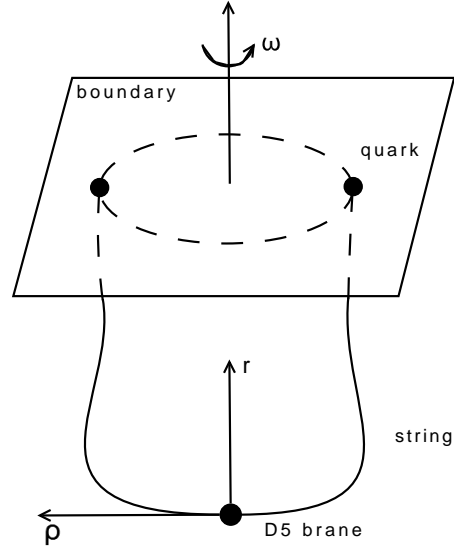


Figure 2: String-brane representation of high spin baryon, the bottom of the strings corresponds to the cusp of the embedding function in Figure 3

$$\mathcal{L} = \sqrt{-\left(\frac{r^2}{R^2}\rho^2\omega^2 - f(r)\right)\left(\frac{1}{f(r)} + \frac{r^2}{R^2}\rho'^2(r)\right)}. \quad (3.1)$$

The equation of motion for $\rho(r)$:

$$\left(\frac{\partial}{\partial\rho(r)} - \frac{\partial}{\partial r}\frac{\partial}{\partial\rho'(r)}\right)\mathcal{L} = 0. \quad (3.2)$$

To solve the above equation of motion, we need two boundary conditions, the values of $\rho(r_e)$ and $\rho'(r_e)$. Since the axial symmetry, $\rho(r_e)$ must vanish. We have $\rho(r_e) = 0$ even if we rotate the hanging strings. However, $\rho'(r_e) \neq 0$ and it need to be defined by other conditions. Since when we rotate the massive strings, the centrifugal force will change the angle ψ shown in figure 1, where $\cot\psi = \rho'(r_e)$.

In fact we determine r_e by the radial FBC at first. From (2.12)(2.13)(2.14), the FBC can be written as

$$\sum_{i=1}^{N_c} \mathcal{L}^{(i)} - \rho'^{(i)} \frac{\partial \mathcal{L}^{(i)}}{\partial \rho'^{(i)}} = \frac{V_5}{(2\pi)^4 \alpha'^2} \frac{\partial \mathcal{V}(r_e)}{\partial r_e}. \quad (3.3)$$

For axial symmetry, we can write

$$\mathcal{L} - \rho' \frac{\partial \mathcal{L}}{\partial \rho'} = \frac{1}{N_c} \frac{V_5}{(2\pi)^4 \alpha'^2} \frac{\partial \mathcal{V}(r_e)}{\partial r_e}. \quad (3.4)$$

The above equation does not include any unknown function since we choose $r = r_e$. This force

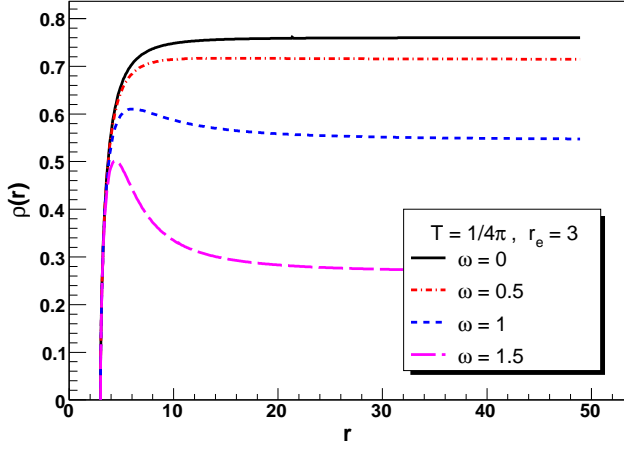


Figure 3: The embedding function $\rho(r)$ at different values of ω when we fixed the r_e

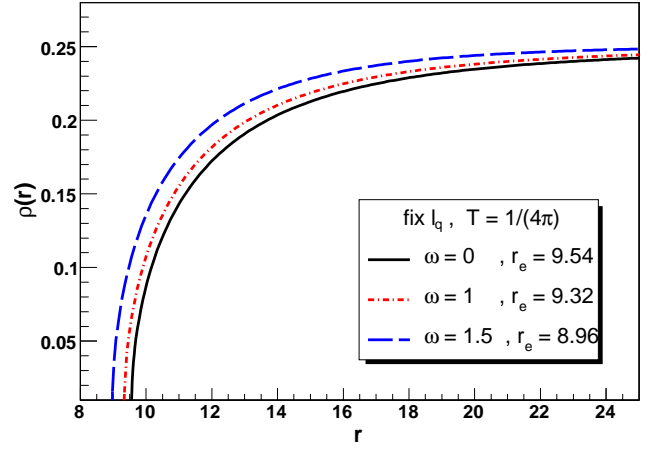


Figure 4: The embedding function $\rho(r)$ at different values of ω when we fixed l_q , $r_\Lambda = 100$

balance condition gives

$$\rho'(r_e) = \frac{R}{r_e f(r_e)^{1/2}} \sqrt{\frac{R^2(r_e^4 - r_0^4)r_e^4}{(r_e^4 + r_0^4)^2 A^2} - 1}, \quad (3.5)$$

where

$$A = \frac{1}{N_c} \frac{V_5}{(2\pi)^4 \alpha'^2} \quad (3.6)$$

This equation gives the constraint about the relation between $\rho'(r_e)$ and r_e . Because the solution $\rho(r)$ depends on the nontrivial boundary condition $\rho'(r_e)$, we can solve the two equations (3.2) (3.5) numerically together.

Solving the equation, we have one free input value of r_e . It also means we can input the length of radial trajectory of the strings $r_\Lambda - r_e$. When the r_e is given, the quarks separation on the cutoff brane l_q can be calculated by the solution $\rho(r)$

$$l_q = 2 \int_{r_e}^{r_\Lambda} \rho'(r) dr = 2\rho(r_\Lambda). \quad (3.7)$$

When ω increases from 0 to finite, the embedding function $\rho(r)$ can be solved as in Figure 3. In this figure, we choose the embedding functions of different baryons with the same r_e . Here, we use the “different”, which means the initial separation between quarks and their energy are different even when we have not rotated them. It also means the interaction potential between quarks are different while $\omega = 0$ for the curves in Figure 3. For baryon of same spin the larger interaction potential also corresponds to the larger boundary quark separation in our confining phase, which will be shown in Figure 8 in next section. Figure 3 teaches us that the strings warp near the horizon but become straight near the boundary, it's reasonable because the compact D5 brane is like a box which transfers the interaction between the strings.

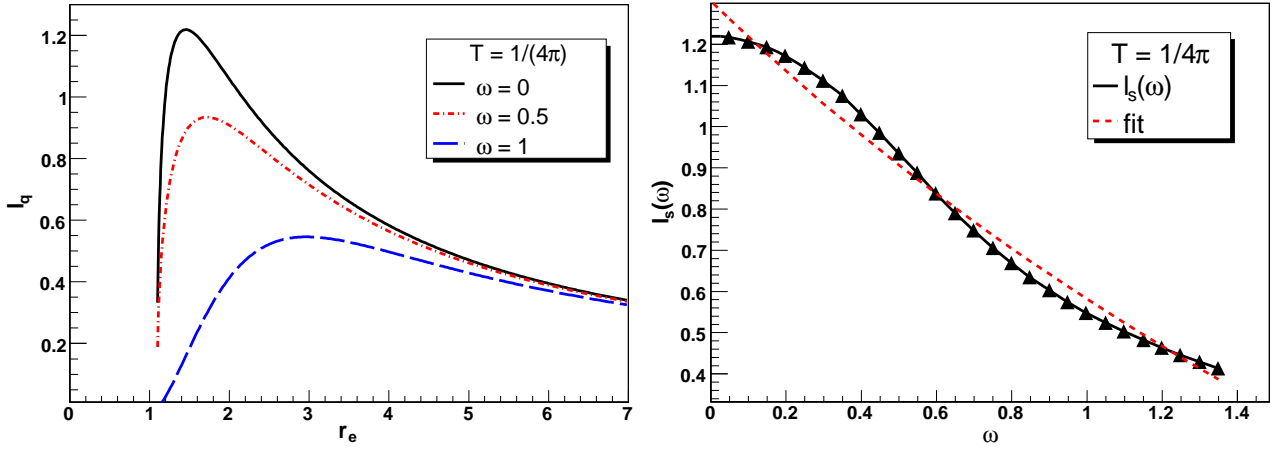


Figure 5: r_e dependence of l_q at different ω values, Figure 6: ω dependence of the screening length, each curve has two branches we choose the right the fit curve is the modified inverse proportion part as the area of stable baryon, $r_\Lambda = 100$ function, $r_\Lambda = 100$

The corresponding configuration of the baryon is shown in Figure 2. The tip of the string becomes lower when we increase ω , to guarantee that the speed of the tip are smaller than speed of light and to make the centrifugal force not too large. Since the bottom part of the string is heavy, at the same centrifugal acceleration, it sticks out in the ρ direction apparently.

If we fix the separation of boundary quarks and stand in the static frame of baryon, the rotating medium will try to separate them and make the connecting string in the bulk longer. We see the result from the solutions in Figure 4. We are interested in the behavior of the l_q as r_e changes. For different values of ω , we plot the r_e dependence of l_q in Figure 5. In this figure, there is an important phenomenon that l_q becomes large at first then turns to be smaller, as we increase the r_e . Actually, for the same l_q , we get two possible values of r_e from the curves in this figure. We consider that the right part of the each curve stands for the stable baryon state and the left part is unstable and we throw it away. It's reasonable because in the right part, r_e becomes small when l_q becomes large, which means that high energy baryon can probe the deeper position in the bulk than low energy baryon if they have same spin. We see that the energy of the stable baryon with same spin must be large if the average separation between the quarks is large in the next section. In another view, for baryons of same spin, the only way to have high energy is to keep the quarks with large separation stable. However, we can introduce high spin to revise this relation between l_q and r_e as shown in this figure. High spin helps to weaken the increase of the l_q as r_e becomes smaller. In our classical picture, rotating strings can contribute more energy.

We define the baryon screening length as the critical quark separation in Figure 5. When ω increases from zero, the screening length seems to decrease like $l_s \propto \frac{1}{\omega}$ in Figure 6. When we fit the curve using

$$l_s = \frac{a}{b\omega + c} - d, \quad (3.8)$$

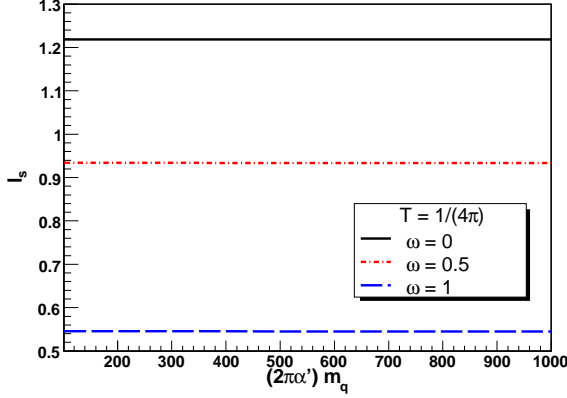


Figure 7: Cut off dependence of the screening length at different values of ω

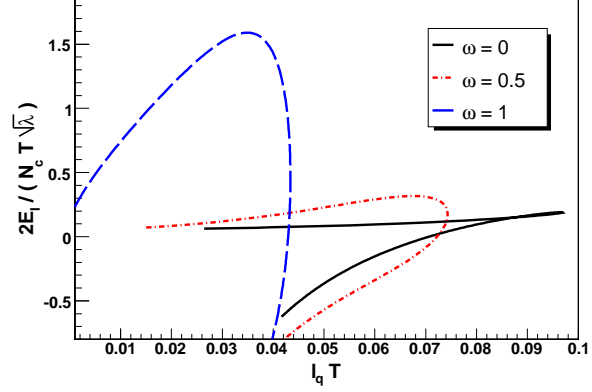


Figure 8: The interaction potential of baryon configuration with a given l_q for several values of the angular velocity ω , $r_\Lambda = 100$. Two branches meets at $l_q = l_s$.

we find the best result is

$$l_s = \frac{0.5}{0.25\omega + 0.25} - 0.44. \quad (3.9)$$

In hot plasma, the screening length depends on the temperature directly and it is different for various hadrons. The smaller screening length of the baryons of higher spin makes them dissociate more easily at a certain temperature in the plasma. The real plasma always become cold very quickly after formation, the high spin baryons appear later than the low spin baryons.

For simplicity, we ignore the backreaction of the cutoff brane. For different values of m_q , the screening length is shown in Figure 7. In this figure, we find that the screening length almost keep the same value while we choose different cutoff. It shows that the screening length is a property of the medium, which is the strongly coupled SYM in this case. Of course, screening lengths are different for baryons with different spins, because in the high spin case, we see the medium rotates if we stand the rest frame of the quarks. When we choose a very large cutoff in the bulk, the bulk theory is more like the SYM. Since the conformality of SYM, the quark scale dependence of screening length is negligible.

4 High spin baryon at nonzero temperature

In section 3, we argue that a high spin baryon can be described by rotating semiclassical strings with the massive brane. In particular, we analyze the screening lengths for different spins. Screening length is considered as the most important signal of quark gluon plasma. Now, we will pay more attention on the property of the baryon itself. In this section, the boundary conditions for stable high spin baryons will be analyzed in detail, and baryon energy and angular momentum will be defined. More evidence of rotating configuration will be given by

the relation of the energy and the angular momentum. We find two branches of the Regge-like behaviors in some conditions.

We want to analyze the boundary condition on the cutoff brane. In section 2, we get the Nambu-Goto action after parameterizing the string world sheet in spacetime:

$$S_{string} = \frac{\mathcal{T}}{2\pi\alpha'} \int_{r_e}^{r_\Lambda} dr \sqrt{-\left(\frac{r^2}{R^2}\rho^2\omega^2 - f(r)\right)\left(\frac{1}{f(r)} + \frac{r^2}{R^2}\rho'^2(r)\right)}. \quad (4.10)$$

Variation of the action gives the boundary term:

$$\frac{\mathcal{T}}{2\pi\alpha'} \frac{\partial \mathcal{L}}{\partial \rho'} \delta \rho|_{r_e}^{r_\Lambda} \quad (4.11)$$

In section 3, we calculate the screening length by considering $\delta\rho(r_\Lambda) = 0$. Because we think that the orbit of the rotating string is exactly a close circle and the radius never changes for the given ω . But $\delta\rho(r_\Lambda) \neq 0$ when we try to change ω . That means baryons with fixed $\rho(r_\Lambda)$ are unstable for different ω . We want to pick up the stable configurations and analyze the ω dependence of the energy and charge. So we choose the boundary condition satisfying:

$$\frac{\partial \mathcal{L}}{\partial \rho'} = 0, \quad (4.12)$$

from which we obtain

$$\frac{1}{4} l_q^2 \omega^2 = \left(1 - \frac{r_0^4}{r_\Lambda^4}\right) \quad (4.13)$$

or

$$\rho'(r_\Lambda) = 0. \quad (4.14)$$

We can easily know the end point of string moves with light speed on the cutoff brane with the first condition (4.13). While the string is orthogonal to the brane with the second condition (4.14).

We now want to give more details about the embedding of the string with angular velocity ω and define properties of baryon with these two boundary conditions. We want to look at the condition (4.13) first. Unfortunately after analyzing a certain $\rho(r)$ with small ω , we can not find a light speed point. Then we look at the condition (4.14). From our numerical result in the section 3, no matter what value of r_e is given, the strings can be always orthogonal to the boundary plane in the infinitely far point in radial direction. However, for our cutoff r_Λ , we have not the infinite point. We can only choose a solution satisfying the orthogonal condition in finite point r_Λ , which corresponds the highest point in Figure 3. Thus we can pick up the string configurations satisfying this orthogonal boundary condition as shown in Figure 18.

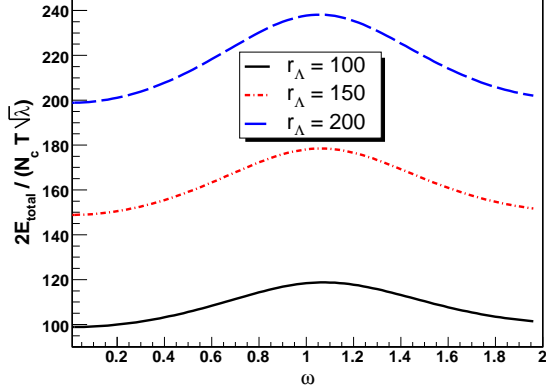


Figure 9: ω dependence of the baryon energy when we fix the r_e

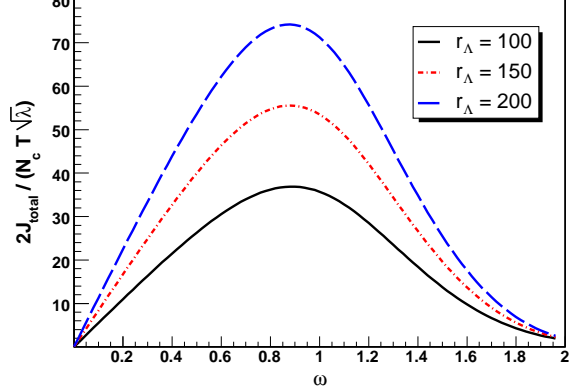


Figure 10: ω dependence of the baryon J charge when we fix the r_e

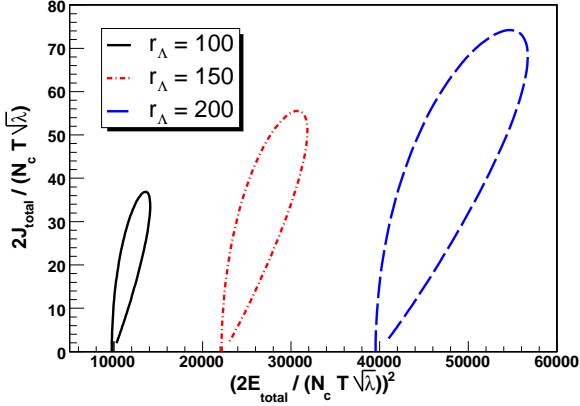


Figure 11: Two branches of Regge-like behavior of baryon when we fix the r_e , the left(right) branch corresponds to smaller(bigger) ω

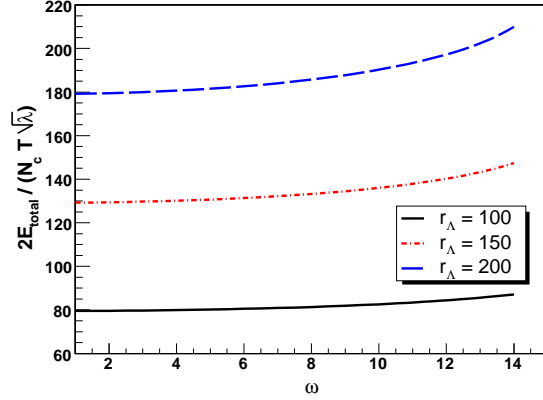


Figure 12: ω dependence of the baryon energy when we fix the l_q on the boundary, three curves stand for the three different cutoffs

Now, we want to give the definition of baryon energy and angular momentum. In spacetime, we write the string Lagrange from the Nambu-Goto action (2.9)

$$L = \frac{1}{2\pi\alpha'} \int_{r_e}^{r_\Lambda} dr \sqrt{-\left(\frac{r^2}{R^2}\rho^2\omega^2 - f(r)\right) \left(\frac{1}{f(r)} + \frac{r^2}{R^2}\rho'^2(r)\right)}. \quad (4.15)$$

The string angular momentum and the energy of the string (we choose positive values) are

$$J_{string} = \frac{\partial L}{\partial \omega} = \frac{1}{2\pi\alpha'} \int_{r_e}^{r_\Lambda} dr \frac{\left(\frac{1}{f(r)} + \frac{r^2}{R^2}\rho'^2(r)\right) \left(\frac{r^2}{R^2}\rho^2\omega\right)}{\sqrt{-\left(\frac{r^2}{R^2}\rho^2\omega^2 - f(r)\right) \left(\frac{1}{f(r)} + \frac{r^2}{R^2}\rho'^2(r)\right)}}, \quad (4.16)$$

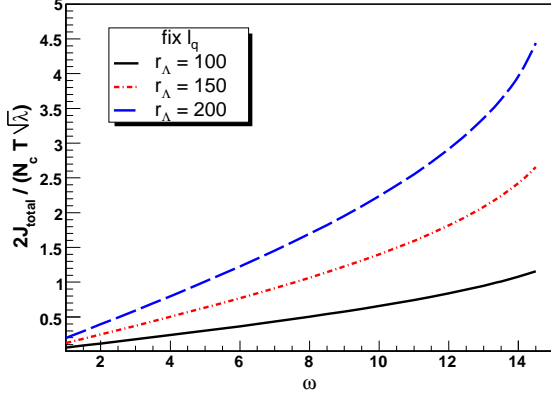


Figure 13: ω dependence of the baryon J charge when we fix the l_q on the boundary, three curves stand for the three different cutoffs

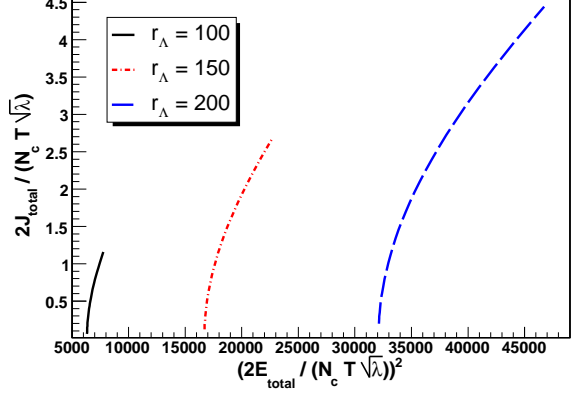


Figure 14: Regge-like behavior of baryon when we fix the l_q on the boundary, three curves stand for the three different cutoffs

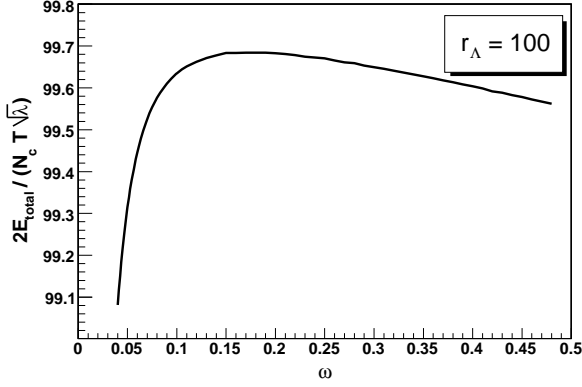


Figure 15: ω dependence of the baryon energy when we choose the orthogonal boundary condition

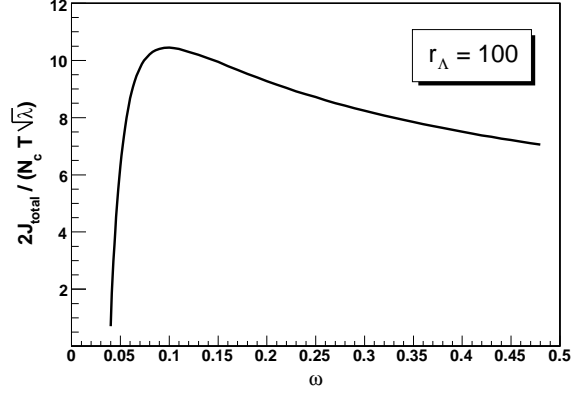


Figure 16: ω dependence of the baryon J charge when we choose the orthogonal boundary condition

and

$$E_{string} = \omega \frac{\partial L}{\partial \omega} - L = \frac{1}{2\pi\alpha'} \int_{r_e}^{r_\Lambda} dr \frac{\left(\frac{1}{f(r)} + \frac{r^2}{R^2} \rho'^2(r) \right) f(r)}{\sqrt{-\left(\frac{r^2}{R^2} \rho^2 \omega^2 - f(r) \right) \left(\frac{1}{f(r)} + \frac{r^2}{R^2} \rho'^2(r) \right)}}. \quad (4.17)$$

The energy of D5 brane is given

$$E_{brane} = \frac{\mathcal{V}(r_e) V_5}{(2\pi)^5 \alpha'^3}. \quad (4.18)$$

The total energy and J charge of the baryon can be defined from the bulk strings and compact D5 brane

$$E_{total} = N_c E_{string} + E_{brane}, \quad (4.19)$$

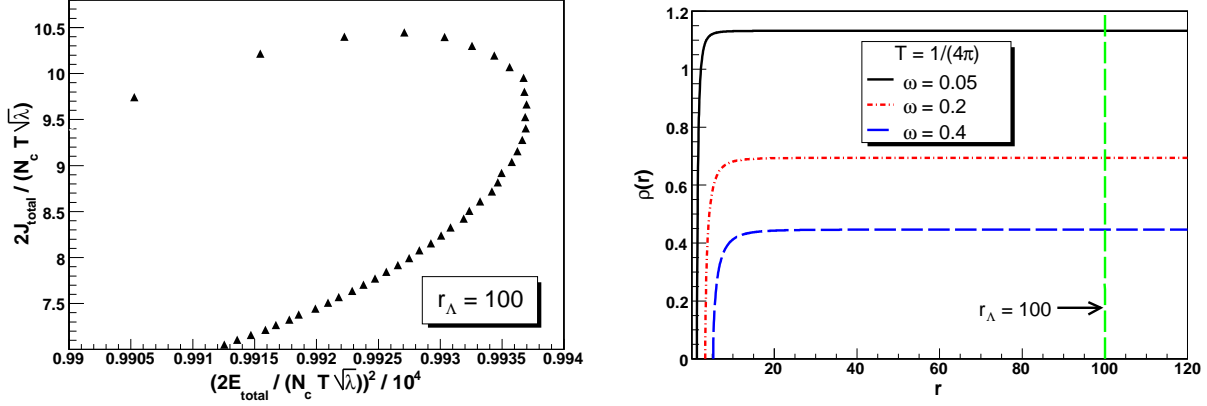


Figure 17: Regge-like behavior of baryon when we choose the orthogonal boundary condition Figure 18: Embedding function with orthogonal boundary condition at different values of ω

and

$$J_{total} = N_c J_{string} + J_{brane}, \quad (4.20)$$

where E_{string} , J_{string} are the string energy and J charge with r_Λ cutoff. Using the above equations (4.16)(4.17)(4.18)(4.19)(4.20), finally we obtain

$$E_{total} = \frac{N_c}{2\pi\alpha'} \int_{r_e}^{r_\Lambda} dr \frac{\left(\frac{1}{f(r)} + \frac{r^2}{R^2} \rho'^2(r) \right) f(r)}{\sqrt{-\left(\frac{r^2}{R^2} \rho^2 \omega^2 - f(r) \right) \left(\frac{1}{f(r)} + \frac{r^2}{R^2} \rho'^2(r) \right)}} + \frac{\mathcal{V}(r_e) V_5}{(2\pi)^5 \alpha'^3}, \quad (4.21)$$

and

$$J_{total} = \frac{N_c}{2\pi\alpha'} \int_{r_e}^{r_\Lambda} dr \frac{\left(\frac{1}{f(r)} + \frac{r^2}{R^2} \rho'^2(r) \right) \left(\frac{r^2}{R^2} \rho^2 \omega \right)}{\sqrt{-\left(\frac{r^2}{R^2} \rho^2 \omega^2 - f(r) \right) \left(\frac{1}{f(r)} + \frac{r^2}{R^2} \rho'^2(r) \right)}} + J_{brane} \quad (4.22)$$

The energy of the hanging string is very large for the mass of free quark, which corresponds to the straight strings energy. To define the interaction potential E_I , we need to subtract the N_c free quarks mass

$$E_q = \frac{N_c}{2\pi\alpha'} \int_{r_0}^{r_\Lambda} dr \left(\frac{1}{\sqrt{1 - \rho^2(r_\Lambda) \omega^2}} \right), \quad (4.23)$$

then the interaction potential can be given

$$E_I = N_c E_{string} - E_q + E_{brane}. \quad (4.24)$$

We find the l_q dependence of the E_I in Figure 8. In this figure, the interaction potential also has a critical behavior at the critical value of $l_q (l_q = L_c)$. For the given l_q we choose the low energy as the energy of stable baryon, and the lower energy also corresponds to the larger r_e in Figure (5).

We investigate the ω dependence of the baryon energy and J charge with three different conditions. The first one, we fix the r_e . The configurations with different ω are shown in Figure 3. We compute the ω dependence of the energy and charge and give the numerical result in figure 9,10. Numerical results about $E_{total}^2 - J_{total}$ relation are shown in Figure 11. In figure 9,10, three different curves correspond to three different cutoffs. We can see the ω dependence of E_{total} and J_{total} . We find that as ω increases from zero, the energy and charge become larger at first and then decrease. The curves have highest points both for the energy and charge. We can explain this phenomena. Two main factors of the variance of energy are angular velocity ω and the rotating radius ρ . The former is dominant at first and the latter is dominant when ω is big enough. The same thing happens to the J charge. We plot the E_{total}^2 dependence of the J_{total} in figure 11. We find that there are two like-Regge branches for the baryon.

The second one, we fix the quarks separation l_q on the boundary brane. It means that we consider the baryons with the same size. We compute the ω dependence of the energy and charge numerically as in Figure 12, 13. We give the Regge-like behavior in Figure 14.

At last, we choose the boundary conditions which we discuss in the beginning of this section. All the hanging string is orthogonal to the cutoff brane. We argue that these configurations are the stable baryons even if we rotate them. So we can pick up them and investigate the ω dependence of E_{total} and J_{total} . The corresponding embedding functions can be shown in Figure 18. The boundary separation $\rho(r_\Lambda)$ becomes small when we increase the ω . Supposing $\omega \sim \rho(r_\Lambda)^n$, from Figure 18, we can set $n = -1.5$. Then we consider a rough and simplest rotating quarks picture on the boundary brane:

$$\frac{\partial E_I(\rho)}{\partial \rho} = m_q \omega^2 \rho \quad (4.1)$$

where the right part is the centrifugal force. Using $\omega \sim \rho(r_\Lambda)^{-1.5}$, we can obtain $E_I \sim \rho^{-1}$. Here, we just ignore the variance of the function $E_I(\rho)$ when ω increases from zero. Let us turn to Figure 8 and look the numerical result. If we fit the curve with $\omega = 0.5$ by using

$$\frac{2E_I}{N_c T \sqrt{\lambda}} = a l_q^c + b, (\rho(r_\Lambda) = l_q) \quad (4.2)$$

we obtain

$$a = -0.060, b = 0.762, c = -1.018 \quad (4.3)$$

while we get

$$a = -0.637, b = 0.949, c = -1.008 \quad (4.4)$$

for the curve with $\omega = 0$. The values of c satisfies $E_I \sim \rho^{-1}$.

We can compute the ω dependence of the energy and charge as in Figure 15, 16. And, we can compute the Regge-like behavior numerically in Figure 17. The curve has two branches and we can fit them by using the linear function respectively. We choose the fit function as

$$\frac{2J}{N_c T \sqrt{\lambda}} = a \left(\frac{2E}{N_c T \sqrt{\lambda}} \right)^2 + b, \quad (4.5)$$

then we get

$$a = 601.606, b = -586.255. \quad (4.6)$$

with small ω corresponding the up branch and

$$a = 652.6, b = -639.9 \quad (4.7)$$

with large ω corresponding the down branch. The values of a can be used to define the Regge slope, with the coefficients before E and J .

5 Discussion and Conclusion

In this paper, we calculate the ω dependence of the baryon screening length in hot plasma. We use the strongly coupled SYM gauge theory to describe the quark gluon plasma and consider the baryon as a probe. By a simple model of baryon in the AdS/CFT frame, we investigate the signature of the baryon probe through the bulk calculation, which is useful to probe properties of strongly coupled gauge theory. In particular, we consider the high spin baryon using the rotating string for the first time, and obtain the ω dependence of the embedding function of a hanging string and baryon screening length. The relation between screening length and spin may be an important experiment signal for the QGP. The energy and charge have been defined for the high spin baryon in our paper. We investigate the Regge-like behavior of the baryons, and give the numerical results in three different conditions in our paper. Among them, we argue that the solutions with orthogonal boundary condition are the best candidates for the baryons with Regge behavior. The most important is that we obtained two branches of Regge-like behavior. The slope is large for large ω as shown in Figure 17. From our result, we get the Regge-like behavior, if we ignore the J_{brane} , which means there is no intrinsic spin of D5 brane. The behaviors are most important properties for baryons in strongly coupled plasma.

However, real relativistic heavy ion collisions quark gluon plasma is different from $\mathcal{N} = 4$ SYM for nonconformality and nonsupersymmetry. To achieve the goal of understanding phenomena in relativistic heavy ion collisions, nonconformality is introduced via a one-parameter deformation of the AdS black hole dual to the hot $\mathcal{N} = 4$ SYM plasma, and robustness with respect to the introduction of nonconformality of five observables of strongly coupled plasmas that have been calculated in $\mathcal{N} = 4$ supersymmetric Yang-Mills (SYM) theory at nonzero temperature has been investigated [19]. The result shows that, in a toy model, the jet quenching parameter and screening length are affected by the nonconformality at the 20 ~ 30% level or less, but the drag and diffusion coefficients for a slowly moving heavy quark are modified by as much as 80%.

On the other hand, considering the QGP be nonsupersymmetric, we can use some other geometry background. We can compactify a space dimension and give antiperiodic boundary condition for the fermions to break supersymmetry completely. In the baryon model in our paper, the compact brane sits at the same point in the AdS space and have a simple action, actually the compact brane is always very heavy and have a nontrivial trajectory in the AdS.

For example, in general case the trajectory of the compact brane in the AdS space (including time direction) can be a plane, but not a line.

That means if we consider different compact D branes, the embedding function of the brane in the geometry can be defined by the DBI action. In this case, the compact brane can be elongated to mimic a string, so the lengths of the string tend to be zero [18]. Properties of baryon can be effected by the brane configuration. Along this way, we can get more interesting properties of the dual baryon model in AdS/CFT and get more information of the baryon probe in the hot plasma.

Acknowledgements

Yang Zhou acknowledges helpful discussions with Tower Wang, Yushu Song, Chaojun Feng, Yi Wang and thanks Xian Gao for kind help. Push Pu would like to thank Jian Deng for numerical discussions and Qun Wang for kind help.

References

- [1] J. M. Maldacena, “The large N limit of superconformal field theories and supergravity,” *Adv. Theor. Math. Phys.* **2**, 231 (1998) [*Int. J. Theor. Phys.* **38**, 1113 (1999)] [arXiv:hep-th/9711200]; E. Witten, “Anti-de Sitter space and holography,” *Adv. Theor. Math. Phys.* **2**, 253 (1998) [arXiv:hep-th/9802150]; S. S. Gubser, I. R. Klebanov and A. M. Polyakov, “Gauge theory correlators from non-critical string theory,” *Phys. Lett. B* **428**, 105 (1998) [arXiv:hep-th/9802109]; O. Aharony, S. S. Gubser, J. M. Maldacena, H. Ooguri and Y. Oz, “Large N field theories, string theory and gravity,” *Phys. Rept.* **323**, 183 (2000) [arXiv:hep-th/9905111].
- [2] S. J. Rey and J. T. Yee, “Macroscopic strings as heavy quarks in large N gauge theory and anti-de Sitter supergravity,” *Eur. Phys. J. C* **22**, 379 (2001) [arXiv:hep-th/9803001].
- [3] J. M. Maldacena, “Wilson loops in large N field theories,” *Phys. Rev. Lett.* **80**, 4859 (1998) [arXiv:hep-th/9803002].
- [4] S. J. Rey, S. Theisen and J. T. Yee, “Wilson-Polyakov loop at finite temperature in large N gauge theory and anti-de Sitter supergravity,” *Nucl. Phys. B* **527**, 171 (1998) [arXiv:hep-th/9803135]; A. Brandhuber, N. Itzhaki, J. Sonnenschein and S. Yankielowicz, “Wilson loops in the large N limit at finite temperature,” *Phys. Lett. B* **434**, 36 (1998) [arXiv:hep-th/9803137]; J. Sonnenschein, “What does the string / gauge correspondence teach us about Wilson loops?,” arXiv:hep-th/0003032.
- [5] O. Kaczmarek and F. Zantow, “Static quark anti-quark interactions in zero and finite temperature QCD. I: Heavy quark free energies, running coupling and quarkonium binding,” *Phys. Rev. D* **71**, 114510 (2005) [arXiv:hep-lat/0503017].

- [6] O. Kaczmarek, F. Karsch, F. Zantow and P. Petreczky, “Static quark anti-quark free energy and the running coupling at finite temperature,” *Phys. Rev. D* **70**, 074505 (2004) [Erratum-ibid. *D* **72**, 059903 (2005)] [arXiv:hep-lat/0406036].
- [7] H. Liu, K. Rajagopal and U. A. Wiedemann, “An AdS/CFT calculation of screening in a hot wind,” *Phys. Rev. Lett.* **98**, 182301 (2007) [arXiv:hep-ph/0607062].
- [8] H. Liu, K. Rajagopal and U. A. Wiedemann, “Wilson loops in heavy ion collisions and their calculation in AdS/CFT,” *JHEP* **0703**, 066 (2007) [arXiv:hep-ph/0612168].
- [9] Q. J. Ejaz, T. Faulkner, H. Liu, K. Rajagopal and U. A. Wiedemann, “A limiting velocity for quarkonium propagation in a strongly coupled plasma via AdS/CFT,” arXiv:0712.0590 [hep-th].
- [10] J.Erdmenger, M.Kaminski, F.Rust “Holographic vector mesons from spectral functions at finite baryon or isospin density” arXiv:0710.0334[hep-th] D.Mateos, S.Matsuura, R.C.Myers and R.M.Thomson Holographic phase transitions at finite chemical potential arXiv:0709.1225[hep-th]
- [11] K. Peeters, J. Sonnenschein and M. Zamaklar, “Holographic melting and related properties of mesons in a quark gluon plasma,” *Phys. Rev. D* **74**, 106008 (2006) [arXiv:hep-th/0606195];
- [12] M. Kruczenski, D. Mateos, R. C. Myers and D. J. Winters, “Meson spectroscopy in AdS/CFT with flavour,” *JHEP* **0307**, 049 (2003) [arXiv:hep-th/0304032];
- [13] O.Antipin, P.Burikham and J.Li “Effective Quark Antiquark Potential in the Quark Gluon Plasma from Gravity Dual Models” hep-ph/0703105
- [14] C. Athanasiou, H. Liu, K. Rajagopal “Velocity dependence of baryon screening in a hot strongly coupled plasma” arXiv:0801.1117 [hep-th].
- [15] A. Karch and E. Katz, “Adding flavor to AdS/CFT,” *JHEP* **0206**, 043 (2002) [arXiv:hep-th/0205236]; M. Kruczenski, D. Mateos, R. C. Myers and D. J. Winters, “Meson spectroscopy in AdS/CFT with flavour,” *JHEP* **0307**, 049 (2003) [arXiv:hep-th/0304032]; J. Babington, J. Erdmenger, N. J. Evans, Z. Guralnik and I. Kirsch, “Chiral symmetry breaking and pions in non-supersymmetric gauge / gravity duals,” *Phys. Rev. D* **69**, 066007 (2004) [arXiv:hep-th/0306018]; M. Kruczenski, D. Mateos, R. C. Myers and D. J. Winters, “Towards a holographic dual of large- $N(c)$ QCD,” *JHEP* **0405**, 041 (2004) [arXiv:hep-th/0311270].
- [16] E. Witten, “Baryons and branes in anti de Sitter space,” *JHEP* **9807**, 006 (1998) [arXiv:hep-th/9805112].
- [17] A. Brandhuber, N. Itzhaki, J. Sonnenschein and S. Yankielowicz, “Baryons from supergravity,” *JHEP* **9807**, 020 (1998) [arXiv:hep-th/9806158].

- [18] Y. Seo, S.J. Sin, “Baryon Mass in medium with Holographic QCD”, arXiv:0802.0568[hep-th]
- [19] H.Liu, K.Rajapopal and Y.Shi, “Robustness and Infrared Sensitivity of Various Observables in the Application of AdS/CFT to Heavy Ion Collisions”, arXiv:0803.3214[hep-ph]